



SACRED HEART RESEARCH PUBLICATIONS

# Journal of Functional Materials and Biomolecules

Journal homepage: [www.shcpub.edu.in](http://www.shcpub.edu.in)



ISSN: 2456-9429

## PREPARATION AND CHARACTERIZATION OF LITHIUM COBALT OXIDE (LiCoO<sub>2</sub>) NANOPARTICLES BY SOL-GEL METHOD

D. Daniel Lawrence<sup>1\*</sup>, E. Ashwini<sup>1</sup>, Dominic Savio C<sup>1</sup>, S. Rahul<sup>1</sup>, Amal George<sup>2</sup>

Received on 22 April 2024, accepted on 15 May 2024,

Published online on June 2024

### Abstract

Lithium-ion batteries are one of the most commercially sought-after energy storages today. Nanocrystalline Lithium cobalt oxide (LiCoO<sub>2</sub>), one of the most promising cathode materials for lithium-ion secondary batteries were synthesized via sol-gel process using aqueous solution of metal nitrates. The chelating agents like oxalic acid and tartaric acid were assisted to get different size and morphology of particle. The optimized size may be achieved through sol-gel processing. The XRD, SEM, UV and FTIR characteristics were studied.

**Keywords:** Lithium-ion batteries, Sol-gel, Chelating agents.

### 1 Introduction

Energy and environmental based issues have become the major areas of concern in the 21<sup>st</sup> century as these factors is directly linked to technological development; therefore, the search for alternative sources of energy continues. Presently the energy economy, which is predominantly based on fossil fuels, is at risk due to the decrease in non-renewable resources and the continuously increasing demand for energy. Furthermore, CO<sub>2</sub> emissions associated with the use of fossil fuels are one of the main causes of global warming, which is becoming an important issue in global energy politics [1, 2]. Accordingly, investments for the exploitation of renewable energy resources are increasing worldwide, with particular attention to solar, wind and battery power systems. Batteries have many advantages as an alternative source of energy storage mechanism [3]. Currently the conventional battery technologies, such as lead-acid and nickel-cadmium batteries, are slowly being replaced by lithium-ion (Li-ion) batteries, fuel-cell technologies and nickel metal hydride batteries. Li-ion battery technology stands as a forerunner and market leader when compared to the other possible energy systems [4].

The main motivation for using this Li-ion battery technology is the fact that lithium is the lightest and most electropositive metallic element and therefore facilitates very

high energy density [5]. Li-ion batteries have been found to be stable over 500 cycles, can be fabricated in different sizes and also require very little maintenance compared to the other battery technologies [6]. Researchers continue to work on many different aspects of this technology such as decreasing the cost, improving the cycling life and increasing the safety. This technology is already being used highly electronics, has recently been introduced to the power tool markets and is entering the hybrid electric-vehicle market making it a serious contender to power the electric cars of the future [7-9].

### 2. Materials and Methods

#### 2.1 Materials

All of the Chemicals used in this work were analytical grade reagents and used without further purification. Lithium nitrate [Li NO<sub>3</sub>], Cobalt nitrate [Co (NO<sub>3</sub>)<sub>2</sub>], Oxalic acid [C<sub>2</sub>H<sub>2</sub>O<sub>4</sub>] and tartaric acid [C<sub>4</sub>H<sub>6</sub>O<sub>6</sub>] were purchased from Merck company. Deionized water was used to prepare all solutions.

#### 2.2 Synthesis of Lithium Cobalt Oxide Nanoparticles

Lithium nitrate and cobalt nitrate was used as reactants. 0.01 mol of lithium and 0.02 mol of cobalt nitrate mixture are dissolved in deionized water and done continuous stirring to get a homogenous solution. Chelating agents such as oxalic acid (0.03 mol) and tartaric acid (0.03 mol) were also added in the dissolved solution and continued 30 minutes of stirring. Then the stirring is continued with heat for another 3 hours to remove water molecules in the dissolved solution and finally the viscous gel is formed. After that the viscous gel is placed into the hot air oven for 3 hours to get dry sample. The obtained pink colour dried sample is calcined at 550° C for 3 hours. Similar procedure is followed for other samples of LiCoO<sub>2</sub>

\*Corresponding author: e-mail [daniel@shcpt.edu](mailto:daniel@shcpt.edu),

<sup>1</sup>PG and Research Department of Physics, Sacred Heart College (Autonomous), Tirupattur – 635 601 Tamilnadu, India.

<sup>2</sup>Department of Mechanical Engineering, University of Saskatchewan, saskatoon S7N 5A9, Canada

[10,11].

### 3. Results and Discussion

The samples of synthesized  $\text{LiCoO}_2$  were characterized by powder XRD analysis, Scanning Electron Microscopy (SEM) morphological analysis, Fourier transform infrared (FTIR) spectral analysis and UV-Vis spectral analysis. From the XRD we found the crystallite size of the materials. The morphology of the  $\text{LiCoO}_2$  were found. The optical studies and functional groups are found successfully.

#### 3.1 Powder X-Ray Diffraction Analysis.

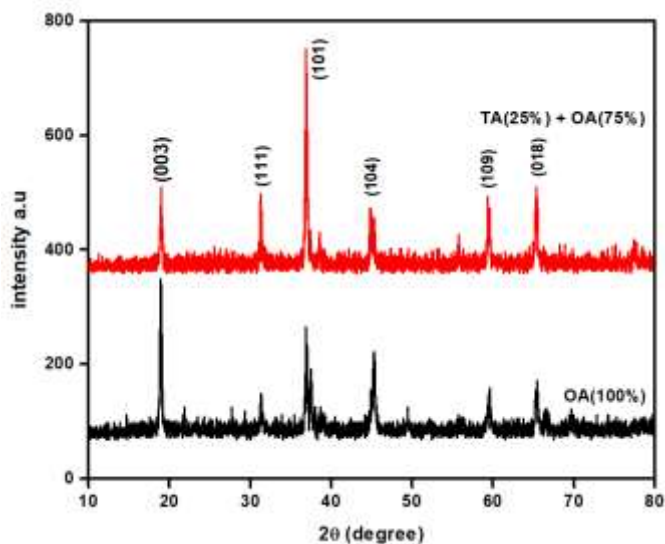


**Figure 1:** XRD patterns of synthesized  $\text{LiCoO}_2$  calcined at  $550^\circ\text{C}$  for 3h using Oxalic Acid (OA) and Tartaric Acid (TA) as chelating agents

The spectrum clearly reveals that there is increase in the intensity of peaks as the concentration of oxalic acid as a chelating agent increases. The miller indices (hkl) values of main diffracted peaks are compared and matched with JCPDF file #77-1370. The observed  $2\theta$  values are 18.96, 36.89, 44.91, 59.46, and 65.35 are associated with (003), (101), (104), (109), and (018) planes. From the analysis it shows that rhombohedral structures are observed. The crystallite size “d” is calculated using the Debye Sherrer formulae

$$d = 0.9\lambda / \beta \cos\theta \dots\dots\dots \text{nm}$$

**Table 1:** Average crystallite size of  $\text{LiCoO}_2$  synthesized with different chelating agents

Sample	Chelating Agents	Average crystallite size in nm
$\text{LiCoO}_2$	Tartaric acid (25%) + Oxalic acid (75%)	21
	Oxalic acid (100%)	19

The average crystallite size of  $\text{LiCoO}_2$  using tartaric acid and oxalic acid as chelating agents is 21 and 19 nm (Table

1). From the table it shows that average crystallite size decreases as the concentration of chelating agent oxalic acid increases and their average crystallite size is found to be 19 nm respectively.

**Table 2:** Lattice constants, c/a ratio, and I (003) / (101) of  $\text{LiCoO}_2$  synthesized using different chelating agents

Sample	Chelating Agents	a (Å)	c (Å)	c/a	I (003) / (101)
$\text{LiCoO}_2$	Tartaric acid (25%) + Oxalic acid (75%)	2.815	14.050	4.991	1.87
	Oxalic acid (100%)	2.815	14.050	4.991	3.1

The integrated intensity ratio of I (003) / (101) peaks has been considered to be a major part signifying the degree of cation ordering in the crystal structure of  $\text{LiCoO}_2$ . It has been proposed that electrochemical performance of cathode material is extremely improved when intensity ratio is higher than 1.2 [16]. The intensity ratio of synthesized  $\text{LiCoO}_2$  using tartaric acid and oxalic acid as chelating agents is 1.1 and 3.1. When the concentration of oxalic acid as a chelating agent increases, the intensity ratio also tends to increase as 1.87 and 3.1 respectively. It clearly reveals that the electrochemical performance of  $\text{LiCoO}_2$  cathode material could be lesser for tartaric acid than oxalic acid as chelating agents [17,18,19].

The particle size and crystalline phase of material plays a major role in cathode performance of lithium batteries. Smaller size distribution resulted in better cycle stability [20]. Thus, from the XRD pattern it concludes that lesser crystalline size of synthesized  $\text{LiCoO}_2$  with oxalic acid as a chelating agent have better electrochemical performance than synthesized  $\text{LiCoO}_2$  with tartaric acid as a chelating agent.

#### 3.2 MORPHOLOGICAL STUDIES

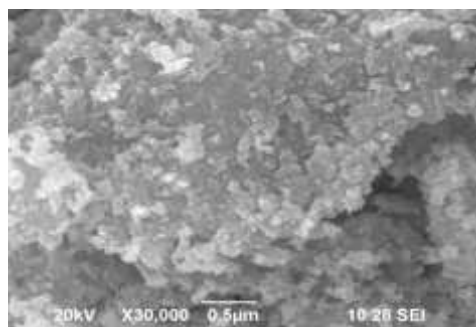


**Figure 2:** SEM image of  $\text{LiCoO}_2$  with tartaric acid (25%) and oxalic acid (75%)

The morphology of  $\text{LiCoO}_2$  calcined at  $550^\circ\text{C}$  for 3hrs are analyzed with SEM images.

Agglomeration is observed from the SEM image (Figure: 2) of synthesized  $\text{LiCoO}_2$  sample. Insufficient lower calcined temperature might be the reason for agglomeration.

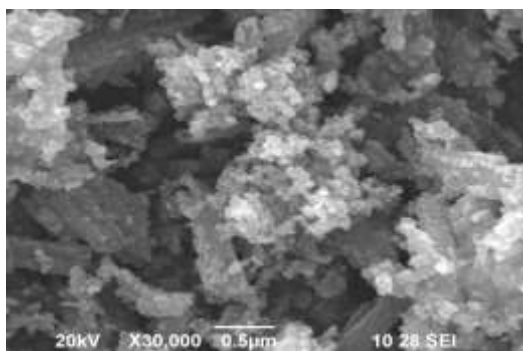


**Figure 3: SEM image of  $\text{LiCoO}_2$  with oxalic acid (100%)**

The SEM image of synthesized  $\text{LiCoO}_2$  sample shows sphere like structure with uniform distribution of particles and also observes little agglomeration. The average particle size of the sample is 105 nm, measured under 0.5  $\mu\text{m}$  in figure: 3 [21].

### 3.3 FTIR STUDIES

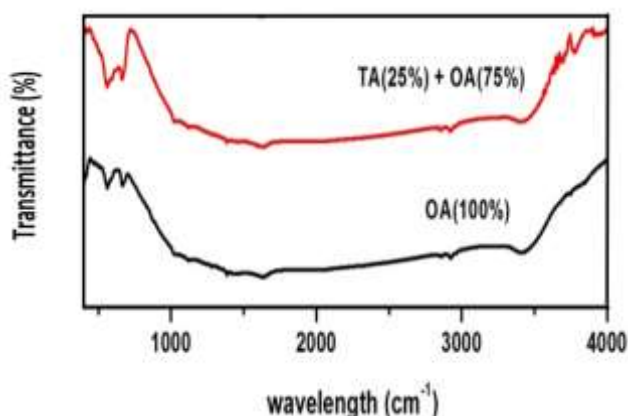


**Figure 4: FTIR spectra of  $\text{LiCoO}_2$  prepared by sol-gel method using oxalic acid and tartaric acid as chelating agents**

The vibrations in the chemical bonding of the sample are recorded through FTIR spectrum. Figure 4 shows FTIR spectra of  $\text{LiCoO}_2$  prepared by sol-gel method using oxalic acid and tartaric acid as chelating agents. The spectra were recorded from 400 - 4000  $\text{cm}^{-1}$  frequency. Functional group analysis predicts that there are two IR active bands. The FTIR bands of  $\text{LiCoO}_2$  are 565, 663, 1397, 2928 and 3398  $\text{cm}^{-1}$ .

The bands observed at 565 and 663  $\text{cm}^{-1}$  frequency confirms the metal oxide peaks. The higher frequency band is located at 1397  $\text{cm}^{-1}$  frequency attributed to asymmetric modes of  $\text{CoO}_2$ . The frequency band 2928  $\text{cm}^{-1}$  is attributed to  $-\text{CH}_3$  stretching is attributed to organic impurity present in the sample. The band 3398  $\text{cm}^{-1}$  is  $-\text{OH}$

stretching vibration. The Vibrational bands are observed and matched with the literature [22-25].

### 3.4 UV-Vis Spectral analysis

The optical absorption spectrum is observed for  $\text{LiCoO}_2$ . The absorption spectrum ranges from 200 - 800 nm. From the absorption spectrum the conductivity band gap energy is calculated. The energy band gap is calculated using the formula

$$E_g = hc/\lambda \text{ (eV)}$$

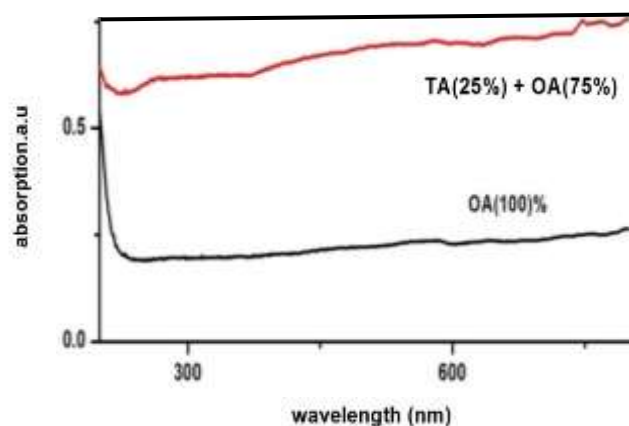


**Figure 5: UV-Vis spectrum of  $\text{LiCoO}_2$  calcined at 550°C, 3h using oxalic acid and tartaric acid as chelating agents**

The Figure 5 shows the UV-Vis spectrum of  $\text{LiCoO}_2$  with oxalic acid and tartaric acid as chelating agents. The absorption spectrum range and its conductivity band gap energy are tabulated below

**Table 3: Absorption range and conductivity band gap energy of  $\text{LiCoO}_2$  synthesized with different chelating agents**

Sample	Chelating Agents	Absorption range (nm)	Band gap energy (eV)
$\text{LiCoO}_2$	Tartaric acid (25%) + Oxalic acid (75%)	218	5.6
	Oxalic acid (100%)	228	5.4

The band gap energy of  $\text{LiCoO}_2$  using tartaric acid and oxalic acid as chelating agents is 5.6 eV and 5.4 eV (Table 3). From the table it shows that band gap energy decreases as the concentration of chelating agent oxalic acid increases and their value is found to be 5.6 & 5.4 eV respectively [26,27,28].

### 4. Conclusion

$\text{LiCoO}_2$  nanocrystalline has been successfully synthesized by sol-gel method. Different samples of  $\text{LiCoO}_2$  are prepared by varying the concentration of oxalic acid and tartaric acid as chelating agents. The dimensions of the  $\text{LiCoO}_2$  nanocrystalline were calculated using Debye's-

scherrer formula. Rhombohedral structure is observed from the XRD pattern. The XRD pattern concludes that lesser crystalline size of synthesized LiCoO<sub>2</sub> with oxalic acid as a chelating agent have better electrochemical performance than synthesized LiCoO<sub>2</sub> with tartaric acid as a chelating agent. The SEM images shows sphere like structure formation with little agglomeration in it. From the SEM images the average crystallite size is found 100 to 300 nm. The FTIR bands of LiCoO<sub>2</sub> are observed and it is also matched with the literature. The band gap energy for the different samples is found.

**Conflict of Interest:** Nil

**Acknowledgement:**

**Reference:**

- [1] Scrosati. B, J. Garche, Lithium batteries: Status, prospects and future, *J. Power Sources*, 195 (2010) 2419-2430.
- [2] M. Armand, Journal of materials issue and challenges facing rechargeable lithium batteries, *Nature*, 414 (2001) 359-367.
- [3] G. N. Lewis, On the Ionization Energy of the Outer Electrons of Atoms and Their Ions, *J. Am. Chem. Soc.*, 192 (1913) 1126-1127.
- [4] M. S. Whittingham, Electrical Energy Storage and Intercalation Chemistry, *Science*, 192 (1976) 1126-1127.
- [5] M. Stanley Whittingham, Lithium batteries and cathode materials, *Chem. Sci. J.*, 104 (2004) 4271-4403.
- [6] M. Wakihara, Recent Developments in Lithium-Ion Batteries, *Mater. Sci. Eng. R Rep.*, 33 (2001) 109-134.
- [7] J. L. Tirado, Inorganic materials for the negative electrode of lithium-ion batteries: state-of-the-art and future prospects, *Mater. Sci. Eng. R Rep.*, 40 (2003) 103-136.
- [8] E. V. Makhonina, Oxide materials as positive electrodes of lithium-ion batteries, *Russ. Chem. Rev.*, 73 (2004) 991-1001.
- [9] S. T. Aruna, A. S. Mukasyan, Combustion synthesis and nanomaterials, *Curr. Opin. Solid State Mater. Sci.* 12 (2008) 44.
- [10] Z. S. Peng, Solubility of vanadyl sulfate in concentrated sulfuric acid solutions, *J. Power Sources*, 72 (1998) 215-220.
- [11] Yuanxiang Gu, Lithium-Cobalt Citrate Precursors in the Preparation of Intercalation Electrode Materials, *J. Phys. Chem. B.*, 109 (2001) 17901-17906.
- [12] Tetsuya Kawamura, Selected papers presented at the 12<sup>th</sup> International Meeting on Lithium Batteries, *J. Power Sources*, 146 (2005) 27-32.
- [13] Masashi Okubo, Nanosize effect on high-rate Li-ion intercalation in LiCoO<sub>2</sub> electrode, *J. Am. Chem. Soc.*, 129 (2007) 7444-7452.
- [14] M. Yoshimura, K. Okada, Proceedings of the Second International Symposium on Soft Solution Processing 2000, *Journal of solid state ionics* 151 (1-4) (2002) 1 - 432.
- [15] Sina Soltan Mohammad, Synthesis and Characterization of LiNiO<sub>2</sub> Nanopowder with Various Chelating Agents, *J. nanomater.*, 91 (2010) 1-8.
- [16] Hailong Chen A, Synthesis and high-rate properties of nanoparticles lithium cobalt oxides as the cathode material for lithium-ion battery, *Electrochem. Commun.*, 4 (2002) 488-491.
- [17] S. Wang, Bismuth-based photocatalysts for solar energy *J. Mater. Chem.*, 2020,8, 24307-24352.
- [18] W. Li, B. Song, A. Manthiram, High-voltage positive electrode materials for lithium-ion batteries, *J. Power Sources* 165 (2007) 491-499.
- [19] Yand-Kook Sun, Synthesis of Spinel LiMn<sub>2</sub>O<sub>4</sub> by the Sol-Gel Method for a Cathode-Active Material in Lithium Secondary Batteries, *Indian Engineering Chemistry*, 36 (1997) 4839-4846.
- [20] Quan-Ming Wang, Thomas C, W. Mak, Novel Honeycomb-Like Layered Structure: The First Isomorphous Triple Salts of Silver Acetylide, *J. Am. Chem. Soc.*, 2000, 122, 31, 7608-7609.
- [21] N. M. Johnson, Z. Yang, Ira Bloom, Z. Zhang, Enabling high temperature and high voltage lithium-ion battery performance through a novel cathode surface-targeted additive, *ACS Appl. Mater. Interfaces.*, 1844341.
- [22] Katsuya Teshima, Environmentally Friendly Growth of Well-Developed LiCoO<sub>2</sub> Crystals for Lithium-Ion Rechargeable Batteries Using a NaCl Flux, *J. Am. Chem. Society.*, 10 (2010) 4471-4475.
- [23] M. Saravanan, M. Ganesan, S. Ambalavanan, An in situ generated carbon as integrated conductive additive for hierarchical negative plate of lead-acid battery, *J. Power Sources*, 251 (2014) 20-29.
- [24] Jinli Yanga, Electrochemical Performance of LiFePO<sub>4</sub>/C via Coaxial and Uniaxial Electrospinning Method, *J. Power Sources.*, 208 (2012) 340-344.

- [25] R. Santhanam, Research progress in high voltage spinel  $\text{LiNi}_{0.5}\text{Mn}_{1.5}\text{O}_4$  material, *J. Power Sources*, 195 (2010) 5442-5445.
- [26] H. Heli, Electronic and transport properties of  $\text{LiCoO}_2$ , *Phys. Chem. Chem. Phys.* (2014) 23412.
- [27] M.-H. Leea, Synthetic optimization of  $\text{Li}[\text{Ni}_{1/3}\text{Co}_{1/3}\text{Mn}_{1/3}]\text{O}_2$  via co-precipitation, *Electrochimica Acta*. 50 (2004) 939-948.
- [28] S.P. Sheu, C.Y. Yao, J.M. Chen, Y.C. Chiou, Proceedings of the Eighth International Meeting on Lithium Batteries, *J. Power Sources* 68 (1997) 533.